JOURNAL OF MATERIALS SCIENCE 23 (1988) 4004–4012

$SrTiO_3$ glass ceramics

Part II *Dielectric properties*

S. L. SWARTZ
Battelle Columbus Division, Columbus, Ohio, USA

A. S. BHALLA, L. E. CROSS
Materials Research Laboratory, Pennsylvania State University, University Park, Pennsylvania 16802, USA

W. N. LAWLESS
CeramPhysics Inc., Westerville, Ohio 43081, USA

The dielectric properties of the strontium titanate aluminosilicate glass-ceramics described in the previous paper have been investigated over the frequency range of 10 to 1000 kHz and temperature range of −170 to 200° C. The dielectric properties were strongly dependent on the crystallization conditions, which determined the amounts of $SrTiO_3$ and secondary crystalline phases, and the microstructure of the glass-ceramics. Room temperature values of the dielectric constant and temperature coefficient varied from 13.5 and +125 p.p.m. $°C^{-1}$ in uncrystallized glass to 47 and −3600 p.p.m. $°C^{-1}$, respectively, in glass-ceramics crystallized for 16 h at 1100° C.

Relatively low dielectric losses ($\tan \delta = 0.002$ at 1 MHz) were observed in uncrystallized glass, and the dielectric losses increased with both frequency and temperature. The dielectric loss at temperatures below −50° C increased upon crystallization of $SrTiO_3$, while the dielectric loss at ambient temperatures (and above) decreased significantly with the crystallization of hexacelsian $SrAl_2Si_2O_8$. The crystallization of titania in glass-ceramics with high crystallization temperatures resulted in large low frequency, high temperature losses, due to Maxwell–Wagner–Sillars effects. In most glass and glass-ceramic samples, a temperature-independent increase of dielectric loss was observed over the frequency range of 10 to 1000 kHz from −50 to 200° C; the cause of these increased losses was not determined.

Maxima in both the dielectric constant and loss appeared at low temperatures (below −100° C), and their magnitudes increased, as the crystallization temperature or time was increased. In the early stages of crystallization, the dielectric constant maxima could be explained on the basis of dielectric mixing between perovskite $SrTiO_3$ and the glassy matrix. However, with higher crystallization temperatures, peaks in the dielectric constant and loss were the result of ferroic effects within the $SrTiO_3$.

1. Introduction

The dielectric properties of glass-ceramics warrant investigation because the crystalline phases and microstructure of glass-ceramics can be controlled by the heat treatment conditions. The possibility thus exists for tailoring of the dielectric properties of a glass-ceramic to those desired for a particular application. The crystallization behaviour and dielectric properties of glass-ceramics with ferroelectric perovskite crystalline phases, such as $BaTiO_3$ [2–5], $PbTiO_3$ [6–14], and $NaNbO_3$ [15–19], have been widely investigated. These studies have demonstrated that both the parent glass composition and heat treatment conditions determine the crystalline phase constitution and microstructure, and thus the dielectric properties of this family of glass-ceramics. The dielectric properties of glass-ceramics with ferroelectric perovskite phases are controlled by such factors as the crystallite size and morphology, the nature and amount of residual glass and secondary phases, crystal clamping, and the connectivity of the high-permittivity perovskite crystals in the low-permittivity glassy matrix.

The development of glass-ceramics for dielectric applications has been hindered by the limited amount of published investigations into the complicated relationships between the crystallization, microstructure, and dielectric properties of glass-ceramics. Perovskite $SrTiO_3$ is a well characterized dielectric material, with a large dielectric constant and extremely low dielectric loss; this suggests that $SrTiO_3$ glass-ceramics may be suitable for a study of the crystallization and dielectric properties of glass-ceramics. $SrTiO_3$ aluminosilicate glass-ceramics have found application as cryogenic capacitive temperature sensors [20–22], and have been proposed for several other cryogenic applications [23–24]. $SrTiO_3$-containing

0022-2461/88 $03.00 + .12

glass-ceramics have also been proposed for ambient temperature applications requiring temperature compensation of the dielectric constant, which is achieved through an appropriate balance between the negative temperature coefficient of $SrTiO_3$ and the positive temperature coefficient of the parent glass [25–26].

Recently, a detailed investigation into the crystallization and dielectric properties of $SrTiO_3$ aluminosilicate glass-ceramics was completed [27], and the crystallization and microstructure of glass-ceramics with a particular $SrTiO_3$ aluminosilicate composition were described in the previous paper [1]. It is the purpose of the present paper to report the dielectric properties of these glass-ceramics, correlating the dielectric results with those of the crystallization study presented in the previous paper. It was hoped that this investigation would lead to an increased understanding, facilitating future efforts at utilizing glass-ceramics for dielectric applications.

2. Experimental procedure

The glass-ceramic samples used in this investigation were identical to those described in the previous paper [1]. Briefly, the glass composition consisted of nominally 65 wt% of $SrTiO_3$, 23 wt% SiO_2, and 12 wt% Al_2O_3. Samples for crystallization studies and subsequent dielectric measurements were discs, approximately 9 mm diameter and 1 mm thick. Prior to crystallization, the glass discs were subjected to a heat treatment at 700° C for 100 h to re-oxidize residual Ti^{3+} that formed during melting. Crystallizations were carried out at temperatures between 800 and 1100° C for times ranging from 15 min to 64 h. Perovskite $SrTiO_3$ was the primary crystalline phase in the glass-ceramics, and secondary crystalline phases included $SrAl_2Si_2O_8$ (hexacelsian or anorthite) and TiO_2 (anatase or rutile). The exact details of the crystalline phase make-up and microstructure of these glass-ceramics were given in reference [1].

Prior to electroding, the glass-ceramic discs were polished parallel with 12 μm alumina. Electrodes consisted of sputtered gold with air-dried silver paint applied to protect the gold and improve electrical contact. Dielectric measurements were made with a Hewlett–Packard 4275A LCR meter at selected frequencies over the range of 10 to 1000 kHz. Temperature capability from -170 to 200° C was achieved with a liquid nitrogen system based on a Delta Design model 2300 temperature control box. Automated measurements spanning the above temperature and frequency ranges were performed utilizing a HP-9816 computer system and associated interfaces. Measurements of capacitance and dissipation factor were made pseudo-continuously on cooling at a rate of $4° C\,min^{-1}$.

Temperature coefficients were calculated as follows: (1) the 1 MHz dielectric constant versus temperature was fit to a ninth-order polynomial; (2) the slopes at 25° C were calculated from the coefficients of the polynomial; and (3) the temperature coefficient was calculated by dividing the slope by the value of the dielectric constant at 25° C. The temperature coefficient calculated in this manner actually corresponded to the temperature coefficient of capacitance because thermal expansion was not taken into consideration. With this qualification, the temperature coefficients of capacitance (TCC) and dielectric constant will be assumed equivalent.

3. Results

3.1. Dielectric constant data

The room temperature dielectric constant of uncrystallized glass was 13.5 with a TCC of 125 p.p.m. $°C^{-1}$. The dielectric constant increased and the TCC became negative upon crystallization of perovskite $SrTiO_3$ with its large dielectric constant (300) and strongly negative TCC (-3600 p.p.m. $°C^{-1}$). The dielectric constant of glass-ceramics crystallized for 1 h increased to a value of 35 as the crystallization temperature was increased to 1000° C, and decreased as the crystallization temperature was further increased to 1100° C. The TCC data were consistent with the dielectric constant data in that the glass-ceramic crystallized at 1000° C had the most negative TCC (-1950 p.p.m. $°C^{-1}$). The increased magnitudes of the dielectric constant and TCC with crystallization temperature up to 1000° C was due to an increased amount of $SrTiO_3$ in the glass-ceramics. With higher crystallization temperatures, a competition between $SrTiO_3$ and other crystalline phases ($SrAl_2Si_2O_8$ and TiO_2) decreased the yield of $SrTiO_3$ in the glass-ceramic, and the magnitudes of the dielectric constant and TCC decreased.

Plots of dielectric constant and TCC against crystallization time at temperatures of 800, 850, and 900° C appear in Fig. 1. These data were consistent with the amount of $SrTiO_3$ with crystallization time, as indicated by the XRD data presented in the previous paper [1]. The dielectric constant remained constant until $SrTiO_3$ was detected by XRD (4 h at 800° C and 20 min at 850° C), and then increased gradually with further crystallization time. A step-function increase of the dielectric constant was observed after 16 h, corresponding to the crystallization of hexacelsian $SrAl_2Si_2O_8$. At 900° C, the crystallization was almost complete after a relatively short time; in these samples, the dielectric constant increased with crystallization time up to 2 h, and then increased at a much slower rate as the crystallization time was further increased. The TCC of glass-ceramics crystallized between 800 and 900° C scaled with the magnitude the dielectric constant, as shown by a plot of TCC against dielectric constant for these glass-ceramics in Fig. 2. As the dielectric constant increased, the TCC decreased as expected. A discontinuity in this curve appeared at a dielectric constant of about 21, corresponding to the crystallization of hexacelsian $SrAl_2Si_2O_8$; this feature was noted earlier with respect to the 850° C crystallized glass-ceramics. The hexacelsian apparently affected the dielectric mixing, resulting in increased magnitudes of the dielectric constant and TCC.

The effect of crystallization time on the dielectric constant as a function of temperature is shown in Figs 3 to 5, as plots of normalized dielectric constant (the dielectric constant divided by the value at 25° C) against temperature for glass-ceramics crystallized for

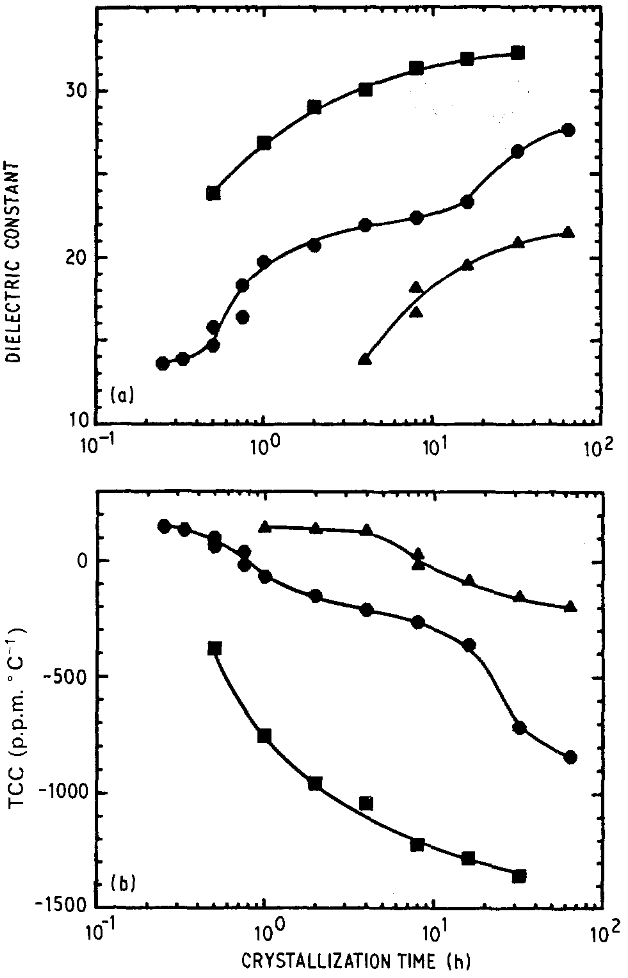

Figure 1 (a) dielectric constant and (b) TCC plotted against crystallization for glass-ceramics crystallized at 800 (▲), 850 (●) and 900 (■) °C.

various times at temperatures of 800, 850, and 900° C. A maximum in the dielectric constant against temperature plot was observed at about −120° C for the glass-ceramic crystallized at 800° C for 16 h. This peak shifted to below −170° C with further crystallization time at 800° C. Similarly, dielectric constant maxima appeared and shifted to lower temperatures as the crystallization time was increased from 0.75 to 2 h at 850° C. The dielectric constant increased with decreasing temperature down to −170° C in glass-ceramics crystallized for longer times at 850° C and at all times at 900° C; dielectric constant peaks occurred at lower temperatures in these samples as indicated by low temperature measurements [28].

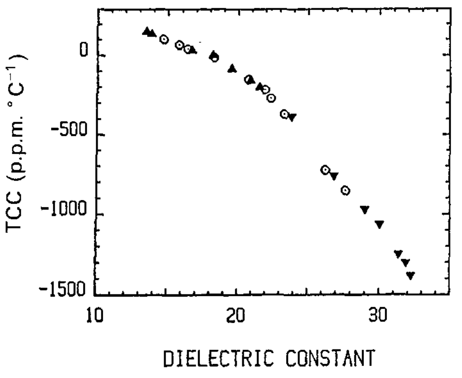

Figure 2 TCC plotted against dielectric constant from dielectric data of glass-ceramics crystallized at 800 (▲), 850 (○) and 900 (▼) °C.

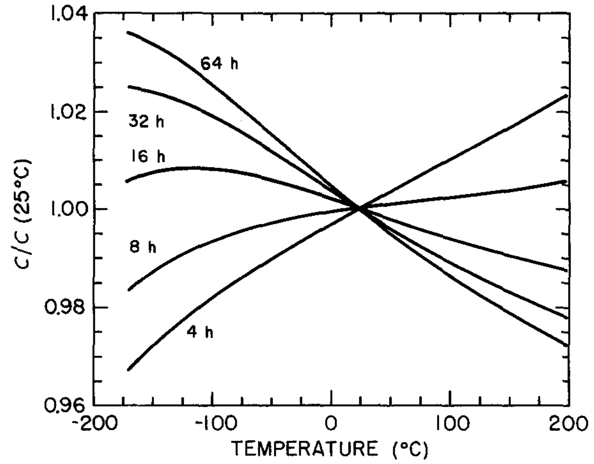

Figure 3 Plot of normalized dielectric constant at 1 MHz (the dielectric constant divided by the value at 25° C) against temperature for glass-ceramics crystallized at 800° C.

The crystallization of $SrTiO_3$ at 1000° C was essentially complete after 1 h, as suggested by room temperature dielectric constant data, and confirmed by XRD [1]. The dielectric constant increased slightly from 33 to 35 during the first hour of crystallization time, and remained constant with further crystallization time. The TCC also increased over the first hour, from −1500 p.p.m. °C^{-1} after 15 min to −1950 p.p.m. °C^{-1} after 1 h. However, the TCC continued to increase with further crystallization time, reaching a value of −2200 p.p.m. °C^{-1} after 16 h, even though room temperature dielectric remained unchanged. The effect of crystallization time at 1000° C is further shown by plots of the normalized dielectric constant against temperature in Fig. 6. Dielectric constant peaks at temperatures below −170° C were also suggested by the shapes of these curves and confirmed by low temperature measurements [28]. The increase of TCC with crystallization time from 1 to 16 h thus resulted from the development of these low temperature dielectric constant peaks.

Dielectric constant and TCC data of the series of glass-ceramics crystallized at 1100° C are presented as plots of dielectric constant and TCC against crystallization time in Fig. 7. The dielectric constant was relatively constant (between 27 and 30) over the first 2 h at this temperature. After 4 h, the dielectric constant increased rapidly with further crystallization time, reaching a plateau value of about 47 after 16 h. The TCC data of glass-ceramics of the 1100° C series followed a similar trend to that of the dielectric constant data. The magnitudes of TCC in glass-ceramics crystallized for 16 and 32 h at 1100° C (about −3800 p.p.m. °C^{-1}) were larger than that measured on a single crystal of $SrTiO_3$ (−3600 p.p.m. °C^{-1}). This would not be possible for straight dielectric mixing beween $SrTiO_3$ and the matrix (assuming single crystal dielectric properties are followed by the $SrTiO_3$ in the glass-ceramic). These data strongly suggest that the low temperature dielectric constant peak was not the result of dielectric mixing.

The temperature dependencies of the dielectric constant of glass–ceramics crystallized at 1100° C were dominated by the presence of dielectric constant peaks

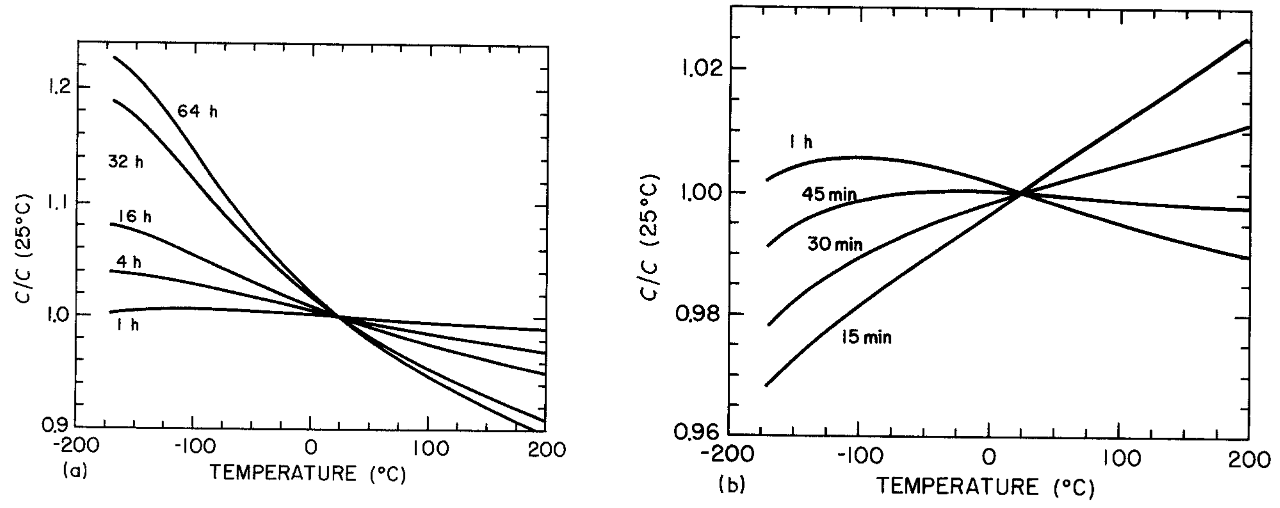

Figure 4 As Fig. 3 for crystallization at 850° C.

below −170° C, which were indicated by low-temperature measurements [28]. The normalized dielectric constant plotted against temperature for glass-ceramics crystallized at 1100° C are compared in Fig. 8. The dielectric constants of glass-ceramics with shorter crystallization times at 1100° C increased with decreasing temperature, suggesting peaks at temperatures much below −170° C. With longer crystallization times, the increase of the dielectric constant with decreasing temperature became more pronounced. After the longer times at 1100° C, the shapes of these curves suggested that the temperature of dielectric constant peaks had increased to just below −170° C; this apparent trend was confirmed [28].

3.2. Dielectric loss data

The dielectric loss of uncrystallized glass was relatively temperature-independent and increased with frequency; at room temperature, dissipation factors were 0.0007 and 0.0016 at 10 and 1000 kHz, respectively. The dielectric loss behaviour of glass-ceramic samples was similar to that of uncrystallized glass; the temperature-independent increase of loss remained upon crystallization. However, the magnitude of the losses were larger and temperature dependence of the losses were significantly different in the glass-ceramics.

The temperature dependence of the dielectric loss in glass-ceramics crystallized at 800 and 850° C are shown by plots of the 1 MHz dissipation factor against temperature in Fig. 9. Dielectric losses of the glass-ceramics with short crystallization times generally increased with frequency and decreased with temperature. As the crystallization time was further increased, the higher temperature losses decreased and the lower temperature losses increased. The increase of the low temperature dielectric loss with crystallization time was especially obvious in the glass-ceramics crystallized at 850° C. The low temperature dissipation factor (−170° C and 1 MHz) increased from about 0.002 to 0.0045 as the crystallization time was increased from 20 min to 64 h. The increase of the low temperature dielectric losses with crystallization time at 800 and 850° C correlated with the increase of the low temperature dielectric constant and suggested a dependence on the amount of $SrTiO_3$ in the glass-ceramic. Another feature observed in the dielectric losses of the 850° C series of glass-ceramics was a sharp decrease of the higher temperature dielectric loss as the crystallization time was increased beyond 16 h, corresponding to the crystallization of hexacelsian $SrAl_2Si_2O_8$. This decrease was especially obvious for the lower frequency (10 and 100 kHz) data. These decreased losses were likely caused by a decrease in the amount of residual glass and thus the migrational component of the dielectric loss. However, despite the lower loss levels, the athermal increase of

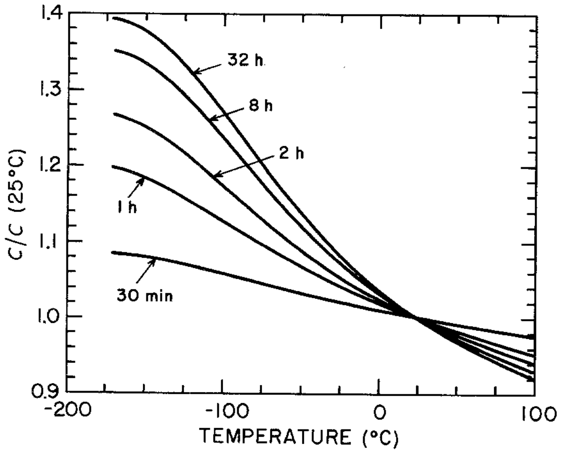

Figure 5 As Fig. 3 for crystallization at 900° C.

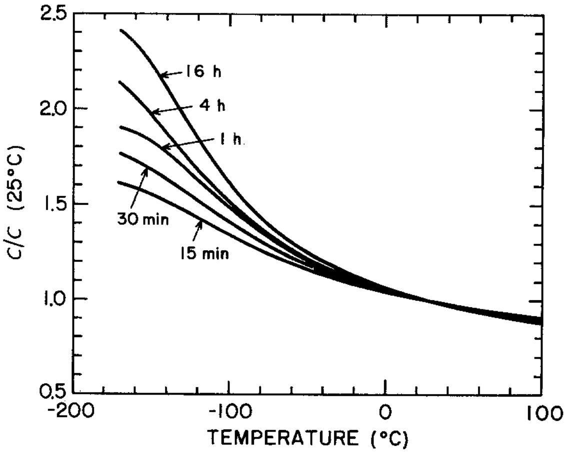

Figure 6 As Fig. 3 for crystallization at 1000° C.

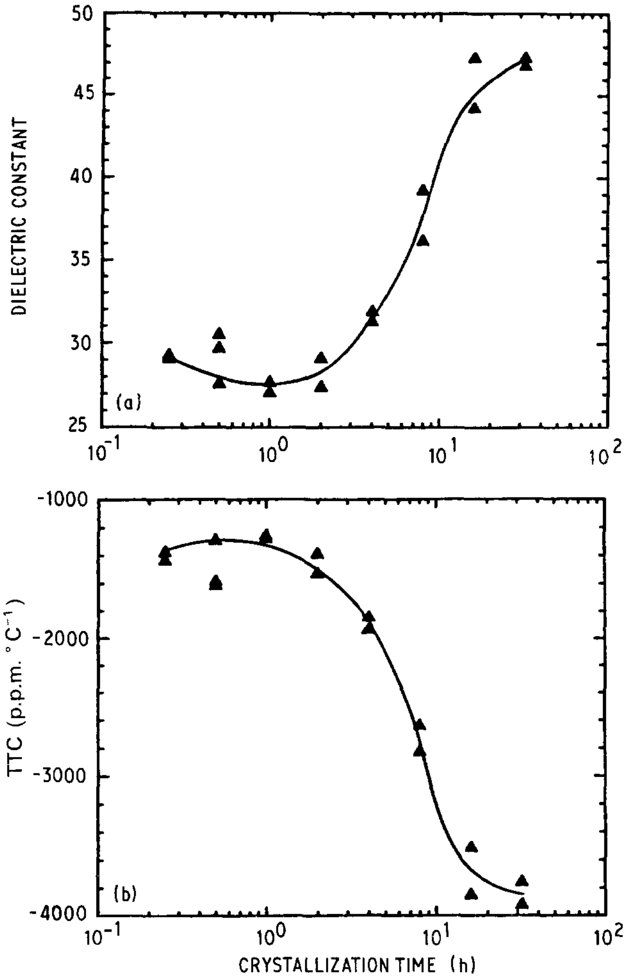

Figure 7 (a) dielectric constant and (b) TCC plotted against crystallization time for glass-ceramics crystallized at 1100° C.

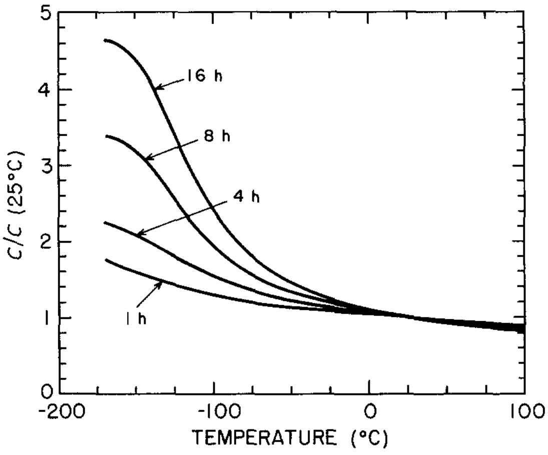

Figure 8 As Fig. 3 for crystallization at 1100° C.

loss with frequency remained intact upon crystallization of hexacelsian.

Dielectric loss spectra of glass-ceramics crystallized at 900 and 1000° C for 1 h are presented in Fig. 10. These data are summarized by two observations: (1) the high temperature dielectric losses were very low, consistent with the presence of hexacelsian $SrAl_2Si_2O_8$; and (2) the low temperature dielectric losses were large and increased with crystallization temperature. The effect of crystallization time on the dissipation factor (1 MHz) as a function of temperature (– 170 to 200° C) of glass-ceramics crystallized at 900° C is shown in Fig. 11. The glass-ceramic crystallized for 30 min displayed somewhat larger high temperature losses, consistent with the incomplete crystallization of hexacelsian in this sample, as indicated by XRD [1]. The high temperature losses of glass-ceramics crystallized for longer times were much lower. The low temperature dielectric losses increased with crystallization time, consistent with the increased dielectric constants. The dielectric loss as a function of temperature of glass-ceramics crystallized at 1000° C were relatively independent of crystallization time, even though the dielectric constant at – 170° C increased from 55 to 84 as the crystallization time was increased from 15 min to 64 h. Apparently the mechanism responsible for the increased magnitude of low temperature dielectric constant peaks did not contribute to the dielectric loss in this temperature range.

Glass-ceramics crystallized at 1100° C displayed large dielectric losses at both low and high temperatures. At higher temperatures, the dielectric loss increased significantly with decreasing frequency. The increase of these losses with crystallization time is shown by plots of the 10 kHz dissipation factor against temperature (0 to 200° C) for glass-ceramics with various crystallization times in Fig. 12. Increased high temperature losses first appeared in glass-ceramics crystallized at 1050° C and corresponded to the crystallization of titania (as anatase or rutile). The titania phase may have been more conductive than the matrix, and thus could have caused the increased high

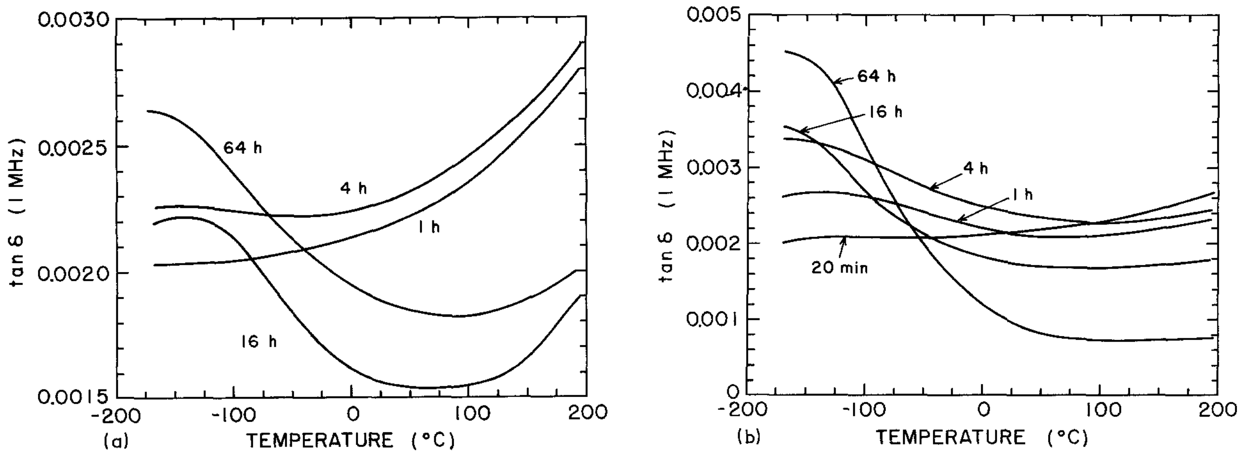

Figure 9 Plot of the 1 MHz dissipation factor against temperature for glass-ceramics crystallized at (a) 800° C and (b) 850° C.

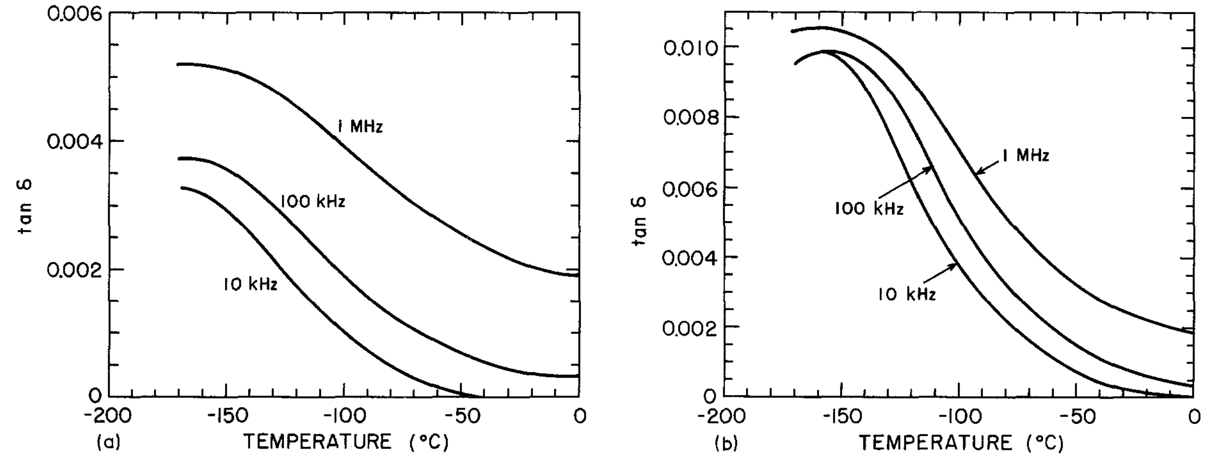

Figure 10 Dielectric loss spectra of glass-ceramics crystallized at (a) 900° C and (b) 1000° C for 1 h.

temperature losses by a Maxwell–Wagner–Sillars mechanism [29]. The increase of these losses with crystallization time at 1100° C was related to microstructure, i.e., the development of the large acicular rutile TiO_2 crystals observed in the SEM micrographs of glass-ceramics crystallized at 1100° C for greater than 2 h [1]. These rutile crystals were shown to be defective, as evidenced by the TEM observation of crystallographic shear planes [1]. The presence of defects (Ti^{3+}) in these rutile crystals would certainly result in high conductivity, and the increased size of the conductive rutile crystals would increase the Maxwell–Wagner–Sillars losses.

Lower temperature dielectric losses of glass-ceramics crystallized at 1100° C also increased with crystallization time, as shown by plots of the 1 MHz dissipation factor against temperature (– 170 to – 100° C), in Fig. 13. The dielectric loss increased in magnitude as the crystallization time was increased, and peaks developed at about – 150° C in glass-ceramics crystallized for the longer times. The development of these loss peaks with crystallization time corresponded to a substantial increase of the dielectric constant in the same temperature range. These loss peaks were frequency dependent and coincided with a large frequency dispersion of the dielectric constant. This is shown in Fig. 14 with plots of the dielectric constant at 10, 100, and 1000 kHz and the dissipation factor at 10, 100, 200, 400, and 1000 kHz against temperature (– 170 to – 100° C) of the glass-ceramic crystallized at 1100° C for 16 h. As the frequency was increased, the dielectric loss peak decreased in magnitude and shifted to higher temperatures. The dispersion of the dielectric constant and the presence of frequency dependent dielectric loss peaks suggest a relaxation type mechanism.

4. Discussion

4.1. Temperature compensation of the dielectric constant

The development of dielectric constant maxima in similar glass-ceramics in the early stages of crystallization was described in an earlier paper [26]. In these glass-ceramics with low $SrTiO_3$ content, maxima in the dielectric constant versus temperature can be predicted on the basis of dielectric mixing between the $SrTiO_3$ and the glassy matrix. This was demonstrated by a modelling study in which the dielectric constant as a function of temperature was calculated from data of single crystal $SrTiO_3$ and uncrystallized glass, using Niesel's approximation [30], valid for high permittivity spheres in a low permittivity matrix

$$k_{12} = 0.25(2A - B) + 0.25(2A - B + 8k_1k_2)^{0.5}$$

where $A = v_1k_1 + v_2k_2$ and $B = v_1k_2 + v_2k_1$. In the above equation, the quantities v and k

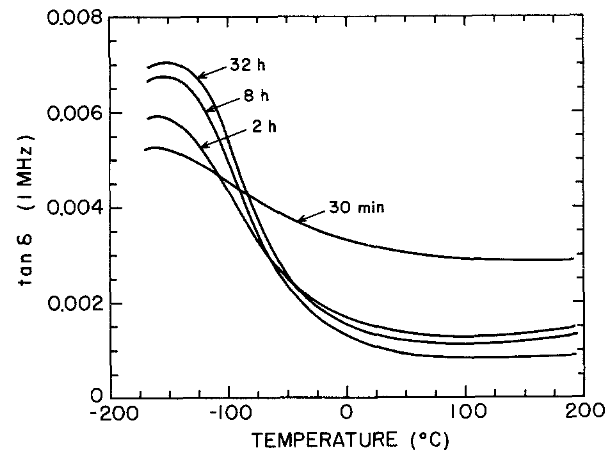

Figure 11 The effect of crystallization time on the dissipation factor (1 MHz) as a function of temperature (– 170 to 200° C) of glass-ceramics crystallized at 900° C.

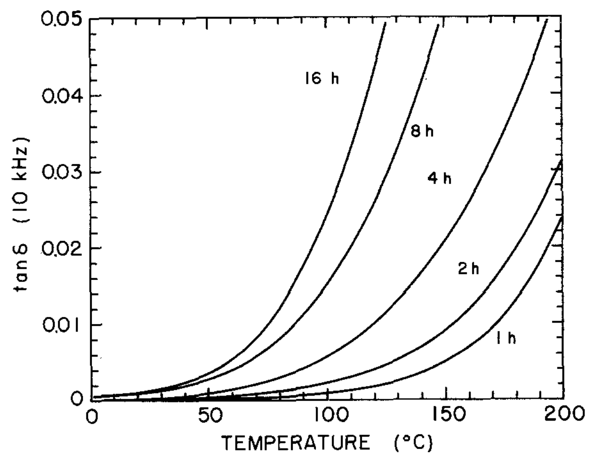

Figure 12 Plot of the 10 kHz dissipation factor against temperature for glass-ceramics for various crystallization times for crystallization at 1100° C.

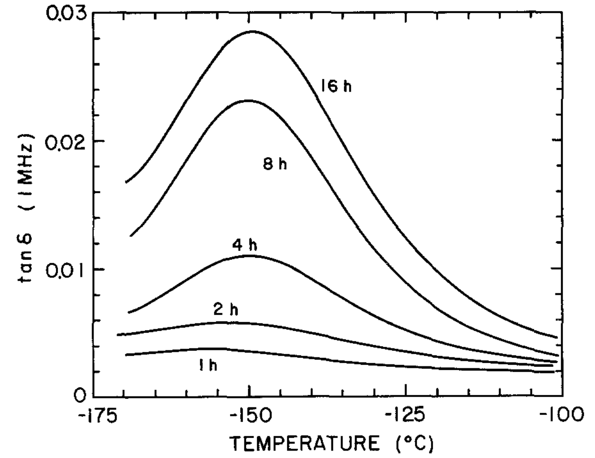

Figure 13 Plot of 1 MHz dissipation factor against temperature for crystallization at 1100° C.

correspond to the volume fractions and dielectric constants, and the subscripts 1, 2, and 12 correspond to the matrix, $SrTiO_3$, and mixture, respectively. This dielectric mixing equation was used in earlier studies of $BaTiO_3$ [1] and $PbTiO_3$ [10] glass-ceramics. The calculated dielectric constant and TCC are plotted against volume fraction $SrTiO_3$ in Fig. 15. This model predicts that the dielectric constant would increase, and the TCC would decrease, becoming negative, as the volume fraction of $SrTiO_3$ was increased. This trend is identical to that observed with both crystallization temperature and time in the present glass-ceramics. A dielectric constant of 16.4 is also predicted for the glass-ceramic with TCC equal to zero, and extrapolation of the data in Fig. 2 gives a similar value of 17.5. The above model predicts that the TCC would be equal to zero with a $SrTiO_3$ volume fraction of 0.074; the dielectric constant as a function of temperature corresponding to this volume fraction, as predicted by this model, is shown in Fig. 16. The modelled temperature dependence gives good qualitative agreement with the observed results; a maximum in the dielectric constant at low temperatures and a minimum at higher temperatures were predicted. This demonstration indicates that the dielectric constant maxima observed in the glass-ceramics with low crystallization temperatures (low $SrTiO_3$ contents) were the result of dielectric mixing.

4.2. Low temperature dielectric behaviour

It was clear from the dielectric measurements presented earlier that the low temperature dielectric constant peaks observed in glass-ceramics with high crystallization temperatures were not the result of simple dielectric mixing between the $SrTiO_3$ and matrix phases, as described above. Further support for this conclusion was obtained from low temperature dielectric measurements of these same glass-ceramics [28]. The temperature range of the loss peaks was insensitive to crystallization conditions and was close to that of the known ferroelastic transition in $SrTiO_3$ [31]. It is possible that the extremely fine crystallite size and/or stresses exerted on the $SrTiO_3$ crystallites by the matrix affected the ferroelastic transition in the $SrTiO_3$. This may have caused the observed relaxation type loss peaks although the nature of this interaction cannot be inferred from the data.

The increased magnitude of the low temperature dielectric constant and loss peaks in the glass-ceramics crystallized for the longer times at 1100° C cannot be related to the amount of $SrTiO_3$ in the glass-ceramic, and must be related to microstructural features: (1) the transformation of the major matrix phase from hexacelsian to anorthite $SrAl_2Si_2O_8$; (2) the development of the large acicular rutile crystals; and (3) an increase of the $SrTiO_3$ crystallite size. The transformation of hexacelsian to anorthite was a gradual change and thus cannot be responsible for the sudden increase of dielectric constant and loss with crystallization times greater than 2 h. The other two factors may have been responsible, by way of the following scenario: (1) the increased $SrTiO_3$ crystallite size may have allowed for a greater contribution of domain wall motion to the dielectric properties; and (2) the development of the acicular rutile crystals, beginning after 4 h at 1100° C, may have altered the mechanical properties of the matrix and affected the interaction of the $SrTiO_3$ with the matrix. These low-temperature dielectric phenomena have recently been described in more detail [28].

4.3. Athermal loss

An interesting feature of these glass-ceramics was the temperature-independent (athermal) increase of dielectric loss observed over the frequency range of 10 kHz to 1 MHz. The upper limit of the frequency range

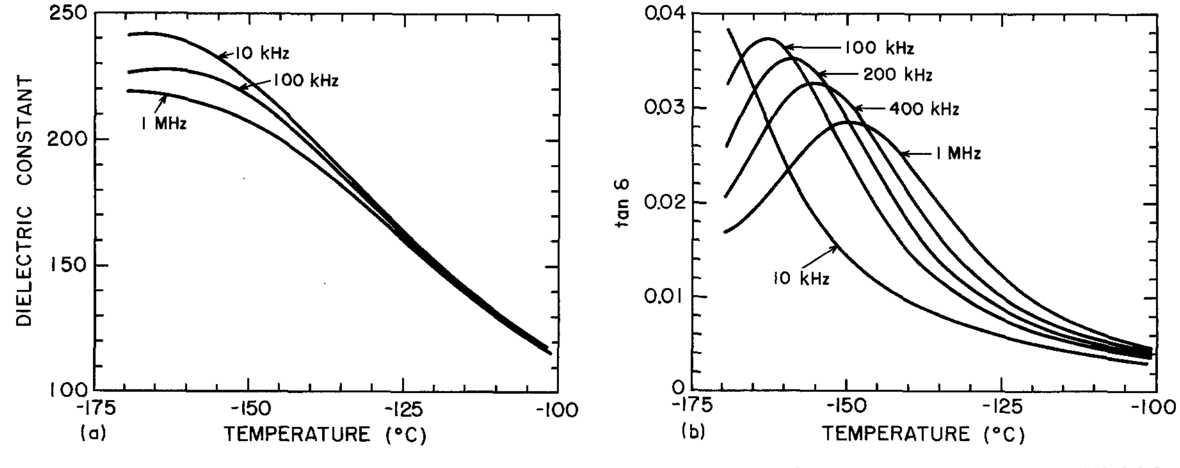

Figure 14 Plot of (a) dielectric constant and (b) 1 MHz dissipation factor against temperature for glass-ceramics crystallized at 1100° C for 16 h.

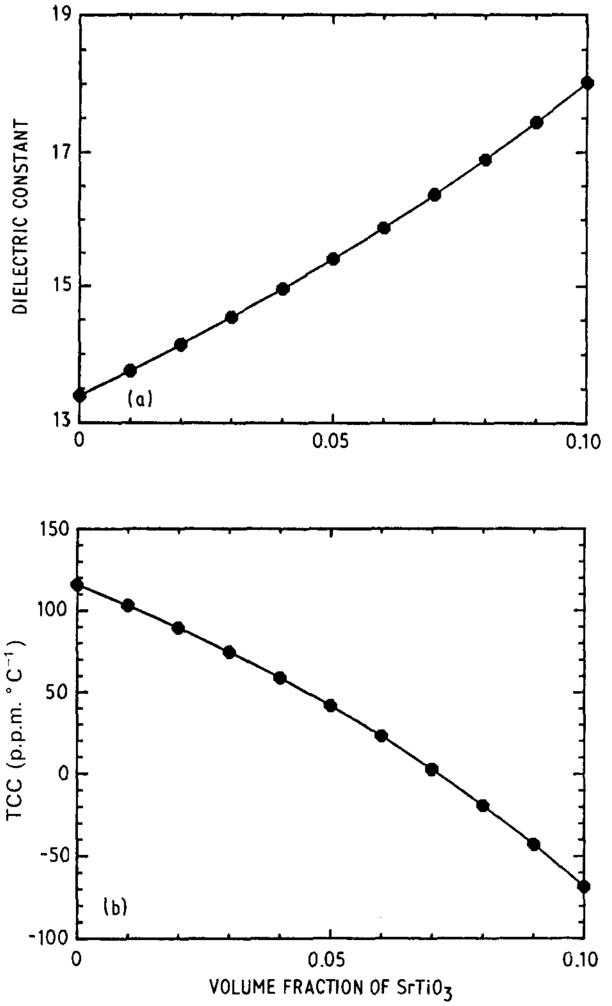

Figure 15 Modelled (a) dielectric constant and (b) TCC plotted against volume fraction $SrTiO_3$ using Niesel's approximation.

of the athermal losses extended well into the microwave region and was not active below 10 kHz [32]. This mechanism dominated the dielectric loss behaviour of uncrystallized glass and certain glass-ceramics over the temperature range of 10 to 500 K. When the other loss mechanisms were present, the athermal loss was obvious in temperature ranges outside of these mechanisms.

Similar athermal increases of dielectric loss with frequency have been observed in alkali-free aluminoborate glasses [33–34]. In calcia-aluminoborate glasses, the athermal loss phenomenon was observed over the frequency range of 100 Hz to greater than 40 GHz [33]. The electrical conductivities of these glasses were low, so that the migrational component of the dielectric loss did not prevent the observation of the athermal loss mechanism at low frequencies. The athermal loss was attributed to the low frequency tail of a vibrational loss mechanism [33]. It was suggested that a vibrational loss mechanism could be extended to lower frequencies by the vibration of entire regions in the glass, i.e., clusters rich in modifying ions [35]. The increased masses of the vibrating species would decrease the vibrational (resonant) frequencies and the wide variety of masses would result in a range of resonant frequencies. Another mechanism was proposed, relating the observed athermal losses to electron hopping between localized energy levels [34, 36].

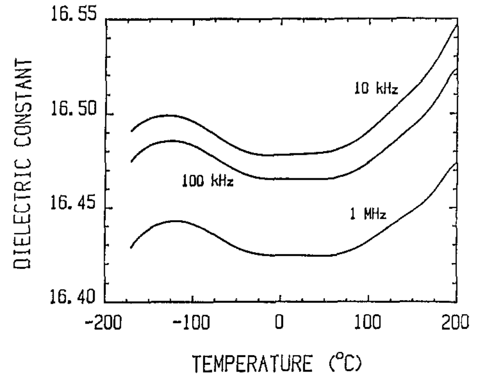

Figure 16 Modelled dielectric constant plotted against temperature for a $SrTiO_3$ volume fraction of 0.074.

Localized energy levels may have been related to structural groups in the glass where charge neutrality was not maintained: (1) a bivalent cation locally associated with only one non-bridging oxygen ion would form an acceptor level: (2) a bivalent cation associated with three or more non-bridging oxygens would form a donor level; and (3) these features would tend to associate with each other and give rise to the possibility of electron hopping transitions.

With regard to the $SrTiO_3$ glass-ceramics of the present study, the insensitivity of the observed athermal loss to crystallization leads to confusion with respect to either of the above explanations. It is clear that the athermal loss in the present glass-ceramics originated from the glass phase. The structure of uncrystallized glass may have been distorted by the presence of the large strontium ions, or by the existence of titanium ion in network-forming (tetrahedral) sites. After crystallization, the structure of residual glass may also have been disturbed, with large compositional heterogeneities. However, the dielectric loss data was insufficient to determine which, if any, of the above mechanisms was responsible for the observed athermal loss behaviour. A comprehensive set of dielectric loss measurements at higher (microwave) frequencies, in conjunction with spectroscopic structural studies, would be necessary to assign a mechanism to the observed athermal loss phenomenon with any confidence.

5. Conclusions

This research has demonstrated that the dielectric properties of these $SrTiO_3$ aluminosilicate glass-ceramics were strongly dependent on microstructure and the nature of the crystalline phases. Contrasting types of dielectric behaviour were observed in glass-ceramics crystallized under various conditions of temperature and time. Specific conclusions are summarized below.

(1) Room temperature values of the dielectric constant and TCC in these glass-ceramics varied from 13.5 and + 125 p.p.m. °C^{-1} in uncrystallized glass to 47 and − 3800 p.p.m. °C^{-1} in the sample crystallized for 16 h at 1100° C.

(2) The dielectric constant and TCC were dependent on the $SrTiO_3$ content in glass-ceramics crystallized below 1000° C; the dielectric constant increased and

the TCC became more negative as the crystallization temperature and time were increased.

(3) In glass-ceramics crystallized between 1000 and 1100° C, the dielectric constant and TCC were affected by microstructure, as dielectric constant peaks developed at low temperatures and their magnitude increased with crystallization time.

(4) High temperature Maxwell–Wagner–Sillars losses were observed in glass-ceramics crystallized at 1100° C; these losses were related to the titania phase, and increased with crystallization time, corresponding to the development of the acicular rutile crystals.

(5) Low temperature dielectric loss peaks were observed and their magnitudes increased with crystallization time for glass-ceramics crystallized from 800 to 900° C, suggesting a dependence on the amount of $SrTiO_3$ in the glass-ceramics. These losses were independent of crystallization time at 1000° C.

(6) The low temperature dielectric losses of glass-ceramics crystallized at 1100° C increased with crystallization time. The glass-ceramics crystallized for 16 and 32 h displayed the highest losses, along with a strong dispersion in the dielectric constant. The low temperature loss behaviour was attributed to ferroic effects within the $SrTiO_3$ crystallites.

(7) A temperature-independent (athermal) increase of dielectric loss with frequency was also observed in these glass-ceramics. The mechanism responsible for the athermal loss could not be determined from the data.

Acknowledgements

Financial support for this work was provided by the US Army Research Office under Contract No. DAAG-82-K-0015. The authors would like to thank Tooser Wilson, Paul Moses, and R. E. Newnham (Materials Research Laboratory, Pennsylvania State University), and W. A. Schulze (New York State College of Ceramics, Alfred University) for their contributions to this research effort.

References

1. S. L. SWARTZ, E. BREVAL, C. RANDALL and B. H. FOX, *J. Mater. Sci.* this issue.
2. A. HERCZOG, *J. Amer. Ceram. Soc.* **47** (1964) 107–115.
3. T. KOKUBO, S. SAKKA and M. TASHIRO, *J. Ceram. Ass. Jpn* **74** (1966) 128–133.
4. T. KOKUBO, C. KUNG and M. TASHIRO, *ibid.* **76** (1968) 89–93.
5. D. HULSENBERG and J. LEHMANN, *Silakattechnik* **34** (1983) 74–76.
6. F. W. MARTIN, *Phys. Chem. Glasses* **6** (1965) 143–146.
7. C. K. RUSSELL and C. G. BERGERON, *J. Amer. Ceram. Soc.* **48** (1965) 162–163.
8. D. G. GROSSMAN and J. O. ISARD *J. Mater. Sci.* **4** (1969) 1059–1063.
9. *Idem, J. Amer. Ceram. Soc.* **52** (1969) 230–231.
10. *Idem, J. Phys. D* **3** (1970) 1058–1067.
11. T. KOKUBO, H. NAGAO and M. TASHIRO, *J. Ceram. Ass. Jpn* **77** (1969) 293–300.
12. T. KOKUBO and M. TASHIRO, *J. Non-Cryst. Solids* **13** (1973/1974) 328–340.
13. M. A. G. C. VAN DE GRAAF, J. C. LODDER and A. J. BURGRAAF, *Glass Techn.* **15** (1974) 143–147.
14. S. M. LYNCH and J. E. SHELBY, *J. Amer. Ceram. Soc.* **67** (1984) 424–427.
15. N. F. BORELLI, A. HERCZOG and R. D. MAURER, *Appl. Phys. Lett.* **7** (1965) 117–118.
16. N. F. BORELLI, *J. Appl. Phys.* **38** (1967) 4243–4247.
17. F. BORELLI and M. M. LAYTON, *J. Non-Cryst. Solids* **6** (1971) 197–212.
18. M. M. LAYTON and A. HERCZOG, *J. Amer. Ceram. Soc.* **50** (1967) 369–375.
19. *Idem, Glass Techn.* **10** (1969) 50–53.
20. W. N. LAWLESS, *Rev. Sci. Instrum.* **42** (1972) 561–566.
21. *Idem, Adv. Cryogenic Eng.* **16** (1971) 261–267.
22. *Idem*, US Patent 3 649 891 (1972).
23. *Idem, Ferroelectrics* **3** (1972) 287–293.
24. *Idem, ibid.* **7** (1974) 379–381.
25. M. MONNERAYE, J. SINDERAT and C. JOUWERSMA, *Glass Tech.* **9** (1968) 70–77.
26. S. L. SWARTZ, M. T. LANAGAN, W. A. SCHULZE, L. E. CROSS and W. N. LAWLESS, *Ferroelectrics* **50** (1983) 313–318.
27. S. L. SWARTZ, PhD Thesis, The Pennsylvania State University, (1985).
28. S. L. SWARTZ, A. S. BHALLA, L. E. CROSS and W. N. LAWLESS, *J. Appl. Phys.* **60** (1986) 2069–2080.
29. R. W. SILLARS, *J. Inst. Elec. Eng.* **80** (1937) 378–394.
30. W. NIESEL, *Ann. Physik* **6** (1952) 336–348.
31. S. L. SWARTZ and M. T. LANAGAN, unpublished data.
32. SAKUDO and UNOKI, *Phys. Rev. Lett.* **26** (1971) 851–853, 1147.
33. A. E. OWEN, *Phys. Chem. Glasses* **2** (1961) 152–162.
34. E. GOUGH, J. O. ISARD and J. A. TOPPING, *ibid.* **10** (1969) 89–100.
35. R. S. PRASAD and J. O. ISARD, *ibid.* **8** (1967) 218–223.
36. V. HALPERN, *Physica* **79B** (1975) 323–349.

Received 23 September 1987
and accepted 26 January 1988